ISSN: 2582-7219

International Journal of Multidisciplinary Research in Science, Engineering and Technology

(A Monthly, Peer Reviewed, Refereed, Scholarly Indexed, Open Access Journal)

Impact Factor: 8.206

Volume 8, Issue 8, August 2025

© 2025 IJMRSET | Volume 8, Issue 8, August 2025| DOI:10.15680/IJMRSET.2025.0808196

ISSN: 2582-7219 | www.ijmrset.com | Impact Factor: 8.206| ESTD Year: 2018|

International Journal of Multidisciplinary Research in Science, Engineering and Technology (IJMRSET)

(A Monthly, Peer Reviewed, Refereed, Scholarly Indexed, Open Access Journal)

Temperature-Dependent Creep Modelling in Orthotropic Composite Shells

Anshu Nagar, Richa Sharma

PhD Student, Dept. of Mathematics, Jaypee Institute of Information Technology, Noida, India

Assistant Professor, Dept. of Mathematics, Jaypee Institute of Information Technology, Noida, India

ABSTRACT: This study aims to demonstrate the application of Seth's transition theory to analyse the time dependent stresses in an orthotropic spherical shell subjected to an external pressure and temperature gradient. Orthotropic materials exhibit different mechanical and thermal properties in three mutually perpendicular directions These materials are increasingly used in high-performance structures such as aerospace components, pressure vessels, and deep-sea submersibles. The governing equilibrium equations are formulated using spherical shell theory, and analytical approach is developed to solve the resulting system. By considering the nonlinear component of the transition state and utilising the principal stresses, the creep stresses are evaluated. On the bases of graphs and numerical computations it can be concluded that topaz has compressive stresses and steel has tensile stresses on the mid-surface of the shell. Therefore, the spherical shell of topaz (orthotropic material) is better in extremely high temperatures without mechanical loading. In contrast, the spherical shell of steel (isotropic material) is better in high-pressure and mechanical loads in the field of design engineering. The results support the advancement of design strategies for orthotropic shell structures subjected to combined thermal and mechanical loading conditions.

Keywords: Spherical shells, temperature, orthotropic materials, creep deformation, transition theory.

I. INTRODUCTION

Shells made of metal or solid materials are predicted to have a wide range of industrial and technological applications. Orthotropic spherical shells are extensively used in aerospace structures, including Satellite antennas and domes, Pressure vessels and fuel tanks and Space habitats and protective enclosures etc. Spherical shells are widely used as pressure vessels in nuclear and chemical plants. Their unique anisotropic behaviour provides enhanced mechanical performance, tailored stress responses, and improved efficiency in solid structures performing under loading conditions.

Analysis of elastic-plastic and creep deformation in Seth [1]. Betton [2] investigated creep deformation in thick-walled shells subjected to internal pressure. Temesgen and others [3] considered a transversely isotropic disc and investigated creep stress with variable density under heat gradient. Saadatfar, Babazadeh and Babaelehi [4] investigated functionally graded piezoelectric revolving disc under thermomechanical and mechanical loads with radiation and convection and found that solar radiation, convection boundary and variable thickness have the significant impact on the disc. Es-Saheb & Fouad [5] employed the finite element approach to analyse the creep deformation in thick-walled cylinder subjected to inner and outer constant load and pressure and found that as the strain rates increases, the pressure on the cylinder's internal surface also increases. Sharma [6] evaluated the stresses in a thin annular transversely isotropic piezoelectric disk with variable thickness and density using mid-zone theory and found that a disk made of barium titanate BaTiO3 (piezoelectric) performs better than a disk made of PZT4 (piezoceramic). Sharma and Nagar [7] employed analytic approach to evaluate the stresses in a functionally graded piezoelectric disc with variable compressibility and variable density and found that annular disc made of PZT-4 is better for the purpose of engineering designs. Godana, Singh and others [8] used Seth's mid-zone idea to generalize strain measure theory for the modelling elastoplastic deformation in a transversely isotropic shell under temperature gradient and consistent pressure and found the stress distribution over the surface of the shell. Bayat and others [9] applied the extended finite element method (XFEM) to researched a fractured orthotropic material under a non-classic thermal shock using the Green-Naghdi (GN) thermos elasticity theory (type II). Jafary & others [10] investigated functionally graded annular plates subjected to different time-dependent loads to improve the design and performance of the porous plate. Vahid Daghigh & others [11] researched the design of FGM spinning disks with variable thickness under extremely high-temperature using

ISSN: 2582-7219 | www.ijmrset.com | Impact Factor: 8.206| ESTD Year: 2018|

International Journal of Multidisciplinary Research in Science, Engineering and Technology (IJMRSET)

(A Monthly, Peer Reviewed, Refereed, Scholarly Indexed, Open Access Journal)

time-dependent creep investigation. Saadatfar & others [12] considered the FG piezoelectric rotating plate with varying thickness to study creep deformation under heat transport including convection and radiation. Matvienko and others [13] investigated the plastic stresses in a rotating disc using mechanical tensile tests and optical microscope techniques and found the plastic resistance reduces with increasing disc width at a constant inner radius, indicating a larger influence from the centrifugal force field. Jafari & Azhari [14] considered the time-dependent cylindrical and spherical shells to analyze the creep deformation with the use of simple HP-cloud mesh-free method. Park & Lim [15] studied a computational model to investigate the creep deformation in the lower head of the reactor pressure vessel using shell theory. Verma & Singh [16] employed concept of transition theory to study creep response of spherical shells with different thickness ratio under pressure and compressibility. Shahi & others [17] employed Seth's transition theory to investigate creep stress in a rotating disc formed of Si-Ti-C-O fibre-bonded CMC and found the spike in strain rates implies that the disc will fracture at the bore next to the inclusion. Sharma and others [18] investigated creep stresses in orthotropic cylinder formed of FGM with internal pressure and external pressure and found both rotation and non-homogeneity have a significant impact on thermal creep strains. Motameni [19] evaluated the elastic-plastic stresses in a rotating disc made up of orthotropic material with variable thickness. Beheshti, A. and others [20] employed a higher-order shell theory for the significant deformation of shells formed of transversely isotropic materials and investigated various instances to demonstrate the functionality of the suggested elements in addition to anisotropy effects. Sharma and Nagar [21] evaluated elastic-plastic stresses in FG isotropic disc to investigate the strength and performance under variable compressibility and variable thickness of the disc. Sharma and Radakovic [22] evaluated stresses and displacement in a rotating disc made up of orthotropic material with stiff rod and found that disc made up of topaz is best for the engineering design purpose.

II. OBJECTIVE OF THE STUDY

In all the studies mentioned in the literature survey stresses in elastic plastic and creep state are assessed for in different solid structures such as thick-walled transversely isotropic spherical shell, transversely isotropic disc, functionally graded piezoelectric revolving disc, functionally graded orthotropic circular cylinder, etc., under different conditions as internal pressure or external pressure, extremely high-temperature, variable thickness, variable compressibility. But no one has evaluated the creep stresses for an orthotropic spherical shell under external pressure and temperature by applying the concept of transition theory.

The aim of the present study is to investigate the strength of the spherical shell composed of orthotropic material when exposed to external pressure and temperature. In this paper, the elastic-plastic deformation in an orthotropic spherical shell exposed to a temperature gradient is investigated by Seth transition theory. The orthotropic spherical shell is considered which is the novelty of this research. The spherical shells of topaz, barite & steel are compared based on their strength and performance under external pressure and thermal loading.

III. MATHEMATICAL FORMULATION

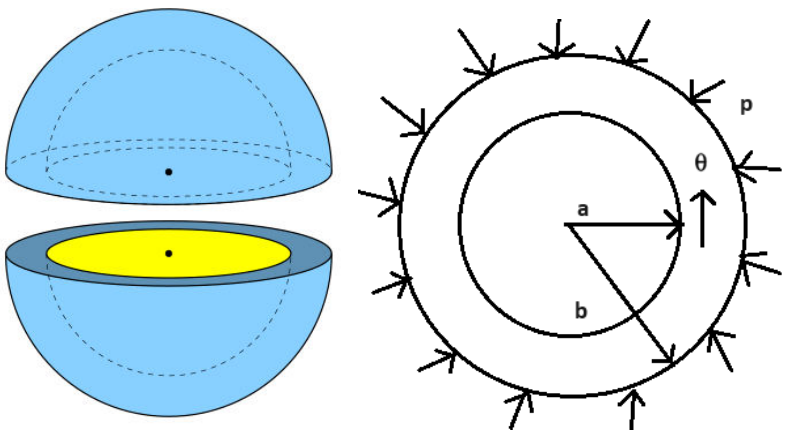

Figure 1: Geometry of the spherical shell.

© 2025 IJMRSET | Volume 8, Issue 8, August 2025| DOI:10.15680/IJMRSET.2025.0808196

ISSN: 2582-7219 | www.ijmrset.com | Impact Factor: 8.206| ESTD Year: 2018|

International Journal of Multidisciplinary Research in Science, Engineering and Technology (IJMRSET)

(A Monthly, Peer Reviewed, Refereed, Scholarly Indexed, Open Access Journal)

Consider a spherical shell with inner radius a and outer radius b, which is exposed to a constant pressure p on its outside surface. The shell's thickness is constant. Figure 1 depicts that the temperature at the spherical shell's centre bore is θ (at $r = a$).

In the form of spherical polar coordinates (r, θ, φ), the displacement co-ordinates u & v are assumed to be $u = r(1-\beta);\ v = 0; w = 0$ (Borah [21]) (1)

where β is a function of variable r where $r = \sqrt{(x^2 + y^2 + z^2)}$

By employing the generalised strain measure (Borah [21]), the principal strain components are given as

$$e_{rr} = \frac{1}{n}[1-(r\beta' + \beta)^n];\ e_{\theta\theta} = e_{\varphi\varphi} = \frac{1}{n}[1-\beta^n]$$
$$e_{r\theta} = e_{\theta\varphi} = e_{\varphi r} = 0. \quad (2)$$

where n is the strain measure; and $\beta' = \frac{d\beta}{dr}$.

The stress-strain relationships for orthotropic materials according to Hooke's Law are expressed as:

$$\sigma_{rr} = c_{11}e_{rr} + c_{12}e_{\theta\theta} + c_{13}e_{\varphi\varphi} - \alpha_1\theta$$
$$\sigma_{\theta\theta} = c_{21}e_{rr} + c_{22}e_{\theta\theta} + c_{23}e_{\varphi\varphi} - \alpha_2\theta$$
$$\sigma_{\varphi\varphi} = c_{31}e_{rr} + c_{32}e_{\theta\theta} + c_{33}e_{\varphi\varphi} - \alpha_3\theta$$
$$\sigma_{r\theta} = \sigma_{\theta\varphi} = \sigma_{\varphi r} = 0. \quad (3)$$

The temperature θ satisfying steady state heat equation $\nabla^2\theta = 0$, with boundary conditions

$\theta = \theta_0$ at $r = a$; $\theta = 0$ at $r = b$

where θ_0 is constant, is given by Timoshenko and Goodier [14]

$$\theta = \frac{\theta_0 a}{(b-a)}\left(\frac{b}{r} - 1\right) \quad (4)$$

Substituting Eq. (2) into Eq. (3), the stresses are as follows:

$$\sigma_{rr} = \frac{c_{11}}{n}[1-\beta^n(1+P)^n] + \frac{(c_{12}+c_{13})}{n}[1-\beta^n] - \alpha_1\theta$$
$$\sigma_{\theta\theta} = \frac{c_{21}}{n}[1-\beta^n(1+P)^n] + \frac{(c_{22}+c_{23})}{n}[1-\beta^n] - \alpha_2\theta$$
$$\sigma_{\varphi\varphi} = \frac{c_{31}}{n}[1-\beta^n(1+P)^n] + \frac{(c_{32}+c_{33})}{n}[1-\beta^n] - \alpha_3\theta \quad (5)$$

where $r\beta' = \beta P$ (P is a β's function and β is r's function), α_1, α_2 and α_3 are coefficients of thermal expansion and θ is temperature.

Equilibrium equations for spherical shell are given by following equations:

$$\frac{\partial\sigma_{rr}}{\partial r} + \frac{1}{rsin\theta}\frac{\partial\sigma_{r\varphi}}{\partial\varphi} + \frac{1}{r}\frac{\partial\sigma_{r\theta}}{\partial\theta} + \frac{2\sigma_{rr}-\sigma_{\theta\theta}-\sigma_{\varphi\varphi}+\sigma_{r\theta}cot\theta}{r} = 0,$$
$$\frac{\partial\sigma_{r\theta}}{\partial r} + \frac{1}{rsin\theta}\frac{\partial\sigma_{\theta\varphi}}{\partial\varphi} + \frac{1}{r}\frac{\partial\sigma_{\theta\theta}}{\partial\theta} + \frac{3\sigma_{r\theta}+(\sigma_{\theta\theta}-\sigma_{\varphi\varphi})cot\theta}{r} = 0,$$
$$\frac{\partial\sigma_{r\varphi}}{\partial r} + \frac{1}{rsin\theta}\frac{\partial\sigma_{\varphi\varphi}}{\partial\varphi} + \frac{1}{r}\frac{\partial\sigma_{\varphi\theta}}{\partial\theta} + \frac{3\sigma_{r\varphi}+2\sigma_{\theta\theta}cot\theta}{r} = 0. \quad (6)$$

Using Eq. 5 and Eq. 6, the following equations of equilibrium are considered

$$\frac{\partial\sigma_{rr}}{\partial r} + \frac{2\sigma_{rr}-\sigma_{\theta\theta}-\sigma_{\varphi\varphi}}{r} = 0,$$
$$\text{or } \frac{\partial\sigma_{rr}}{\partial r} - \frac{2(\sigma_{rr}-\sigma_{\theta\theta})}{r} = 0. \quad (7)$$

Using equations (5) and (7), the nonlinear differential equation is obtained as

$$\beta^{n+1}P(P+1)^{n-1}\frac{dP}{d\beta} = c_{11}\beta^n(P+1)^n - (c_{12}+c_{13})\beta^n p + 2\left[\frac{(c_{11}-c_{21})}{n}[1-\beta^n(1+P)^n] + 2(c_{12}+c_{13}-c_{22}-c_{23})\frac{(1-\beta^n)}{n} - (\alpha_1-\alpha_2)\theta\right\} + \frac{\alpha_1\theta_0 ab}{(b-a)} \quad (8)$$

The following boundary conditions are considered at internal and external surfaces of the shell

$$\sigma_{rr} = 0 \quad at \quad r = a$$
$$\sigma_{rr} = -p \quad at \quad r = b. \quad (9)$$

IV. TRANSITION FROM PLASTIC TO CREEP

Seth's mid-zone theory states that the transition from plastic to creep takes place at the transformation point $P \to -1$ (Borah [21]). For estimating the plastic and creep stresses, the transition function R is considered as

$$R = \sigma_{rr} - \sigma_{\theta\theta} = \left(\frac{c_{11}-c_{21}}{n}\right)(1-\beta^n(1+P)^n) + \frac{(c_{12}+c_{13}-c_{22}-c_{23})}{n}(1-\beta^n) - (\alpha_1-\alpha_2)\theta \quad (10)$$

ISSN: 2582-7219 | www.ijmrset.com | Impact Factor: 8.206| ESTD Year: 2018|

International Journal of Multidisciplinary Research in Science, Engineering and Technology (IJMRSET)

(A Monthly, Peer Reviewed, Refereed, Scholarly Indexed, Open Access Journal)

Taking logarithmic differentiation of equation (8), we get

$$\frac{dlogR}{dr}=\frac{\left(\frac{c_{11}-c_{21}}{n}\right)\left[-\frac{n}{r}\beta^{n+1}P(P+1)^{n-1}\frac{dP}{d\beta}-\frac{n}{r}\left(\frac{r}{r_2}\right)^k\beta^nP(P+1)^n\right]+\frac{(c_{12}+c_{13}-c_{22}-c_{23})}{n}\left(-\frac{n}{r}\beta^nP\right)+(\alpha_1-\alpha_2)\frac{\alpha_1\theta_0ab}{(b-a)r^2}}{\left(\frac{c_{11}-c_{21}}{n}\right)(1-\beta^n(1+P)^n)+\frac{(c_{12}+c_{13}-c_{22}-c_{23})}{n}(1-\beta^n)-(\alpha_1-\alpha_2)\theta} \tag{11}$$

Replacing $\frac{dP}{d\beta}$ value from equation (7) in equation (10) and using the transition point $P\rightarrow -1$, we find

$$\frac{dlogR}{dr}=\frac{\left(\frac{-n(c_{11}-c_{21})(c_{12}+c_{13})}{rc_{11}}\right)\beta^n+\frac{2(c_{11}-c_{21})^2}{r}+\frac{(c_{11}-c_{21})(c_{12}+c_{13}-c_{22}-c_{23})}{rc_{11}}(1-\beta^n)}{\frac{-2(\alpha_1-\alpha_2)\theta\frac{(c_{11}-c_{21})n}{rc_{11}}+-2\alpha_1\theta_0ab\frac{(c_{11}-c_{21})n}{rc_{11}}+(c_{12}+c_{13}-c_{22}-c_{23})(1-\beta^n)+\frac{(\alpha_1-\alpha_2)\theta_0abn}{(b-a)^2}}{\frac{(c_{12}+c_{13}-c_{22}-c_{23})}{n}(1-\beta^n)-(\alpha_1-\alpha_2)\theta}} \tag{12}$$

Taking asymptotic value of $\beta=\frac{D}{r}$ as $P\rightarrow -1$, D is constant.

$$\frac{dlogR}{dr}=\frac{\left(\frac{-n(c_{11}-c_{21})(c_{12}+c_{13})}{rc_{11}}\right)\left(\frac{D}{r}\right)^n+\frac{2(c_{11}-c_{21})^2}{r}+\frac{(c_{11}-c_{21})(c_{12}+c_{13}-c_{22}-c_{23})}{rc_{11}}\left(1-\left(\frac{D}{r}\right)^n\right)}{\frac{-2(\alpha_1-\alpha_2)\theta\frac{(c_{11}-c_{21})n}{rc_{11}}+-2\alpha_1\theta_0ab\frac{(c_{11}-c_{21})n}{rc_{11}}+(c_{12}+c_{13}-c_{22}-c_{23})\left(1-\left(\frac{D}{r}\right)^n\right)+\frac{(\alpha_1-\alpha_2)\theta_0abn}{(b-a)^2}}{\frac{(c_{12}+c_{13}-c_{22}-c_{23})}{n}\left(1-\left(\frac{D}{r}\right)^n\right)-(\alpha_1-\alpha_2)\frac{\theta_0a}{(b-a)}\left(\frac{b}{r}-1\right)}} \tag{13}$$

$$\frac{dlogR}{dr}=G,\quad logR=\int Gdr+logA$$

$$R=Ae^{\int Gdr}=AH \tag{14}$$

Where $H=e^{\int Gdr}$ and

$$G=\frac{\left(\frac{-n(c_{11}-c_{21})(c_{12}+c_{13})}{rc_{11}}\right)\left(\frac{D}{r}\right)^n+\frac{2(c_{11}-c_{21})^2}{r}+\frac{(c_{11}-c_{21})(c_{12}+c_{13}-c_{22}-c_{23})}{rc_{11}}\left(1-\left(\frac{D}{r}\right)^n\right)}{\frac{-2(\alpha_1-\alpha_2)\theta\frac{(c_{11}-c_{21})n}{rc_{11}}-2\alpha_1\theta_0ab\frac{(c_{11}-c_{21})n}{rc_{11}}+(c_{12}+c_{13}-c_{22}-c_{23})\left(1-\left(\frac{D}{r}\right)^n\right)+\frac{(\alpha_1-\alpha_2)\theta_0abn}{(b-a)^2}}{\frac{(c_{12}+c_{13}-c_{22}-c_{23})}{n}\left(1-\left(\frac{D}{r}\right)^n\right)-(\alpha_1-\alpha_2)\frac{\theta_0a}{(b-a)}\left(\frac{b}{r}-1\right)}} \tag{15}$$

Substituting the value from Equation (14) in the equation of equilibrium (7) and integrating, we have

$$\sigma_{rr}=\int\frac{2AH}{r}dr+B \tag{16}$$

From eqn. (10) and (16), we get

$$\sigma_{\theta\theta}=\int\frac{2AH}{r}dr-AH+B \tag{17}$$

After applying boundary conditions (9), we have

$$0=2\left[A\int\frac{H}{r}dr\right]_{r=a}+B \tag{18}$$

$$-p=2\left[A\int\frac{H}{r}dr\right]_{r=b}+B \tag{19}$$

After solving Eqn. (18) and (19), we obtained

$$A=\frac{-p}{2\left[\int\frac{H}{r}dr\right]_{r=b}-2\left[\int\frac{H}{r}dr\right]_{r=a}}$$

$$B=\frac{p}{\left[\int\frac{H}{r}dr\right]_{r=b}-\left[\int\frac{H}{r}dr\right]_{r=a}}\left[\int\frac{H}{r}dr\right]_{r=a} \tag{20}$$

Using equations (16), (17) and (20), we have

$$\sigma_{rr}=\frac{p\left(-\int\frac{H}{r}dr+\left[\int\frac{H}{r}dr\right]_{r=a}\right)}{\left[\int\frac{H}{r}dr\right]_{r=b}-\left[\int\frac{H}{r}dr\right]_{r=a}};\quad \sigma_{\theta\theta}=\frac{p\left(-\int\frac{H}{r}dr+\left[\int\frac{H}{r}dr\right]_{r=a}+H\right)}{\left[\int\frac{H}{r}dr\right]_{r=b}-\left[\int\frac{H}{r}dr\right]_{r=a}} \tag{21}$$

The subsequent non-dimensional components are assumed as

$$R=\frac{r}{b};\ R_0=\frac{a}{b};\ T_{rr}=\frac{\sigma_{rr}}{p};\ T_{\theta\theta}=\frac{\sigma_{\theta\theta}}{p};\ \Theta=\frac{\theta_0(\alpha_1-\alpha_2)}{p} \tag{22}$$

In non-dimensional form,

$$T_{rr}=\frac{\left(-\int\frac{H_1}{R}dR+\left[\int\frac{H_1}{R}dR\right]_{R=R_0}\right)}{\left[\int\frac{H_1}{R}dR\right]_{R=1}-\left[\int\frac{H_1}{R}dR\right]_{R=R_0}};\ T_{\theta\theta}=\frac{\left(-\int\frac{H_1}{R}dR+\left[\int\frac{H_1}{R}dR\right]_{R=R_0}+H_1\right)}{\left[\int\frac{H_1}{R}dR\right]_{R=1}-\left[\int\frac{H_1}{R}dR\right]_{R=R_0}} \tag{23}$$

Where $H_1=e^{\int G_1bdR}$ and

© 2025 IJMRSET | Volume 8, Issue 8, August 2025| DOI:10.15680/IJMRSET.2025.0808196

ISSN: 2582-7219 | www.ijmrset.com | Impact Factor: 8.206| ESTD Year: 2018|

International Journal of Multidisciplinary Research in Science, Engineering and Technology (IJMRSET)

(A Monthly, Peer Reviewed, Refereed, Scholarly Indexed, Open Access Journal)

$$G_1 = \frac{\left(\frac{-n(c_{11}-c_{21})(c_{12}+c_{13})}{bRc_{11}}\right)\left(\frac{D}{bR}\right)^n + \frac{2(c_{11}-c_{21})^2}{bR} + \frac{(c_{11}-c_{21})(c_{12}+c_{13}-c_{22}-c_{23})}{bRc_{11}}\left(1-\left(\frac{D}{bR}\right)^n\right) - 2\Theta p\frac{(c_{11}-c_{21})n}{bRc_{11}} - 2\Theta pbR_0\frac{(c_{11}-c_{21})n}{Rc_{11}} + (c_{12}+c_{13}-c_{22}-c_{23})\left(1-\left(\frac{D}{bR}\right)^n\right) + \frac{bR_0n\Theta p}{(1-R_0)^2}}{\frac{(c_{12}+c_{13}-c_{22}-c_{23})}{n}\left(1-\left(\frac{D}{bR}\right)^n\right) - \frac{\Theta pR_0}{(1-R_0)}\left(\frac{1}{R}-1\right)}$$

V. NUMERICAL EVALUATION

Table 1: Elastic constants values of orthotropic materials (topaz & barite) and isotropic material (steel).

Elastic constants $c_{ij}\left(in\ 10^{11}\frac{N}{m^2}\right)$	c_{11}	c_{12}	c_{13}	c_{21}
Topaz (Orthotropic)	2.813	1.258	0.846	1.258
Barite (Orthotropic)	0.907	0.273	0.275	0.273
Steel (isotropic)	2.908	1.27	1.27	2.908

To observe the effect of temperature and pressure on spherical shell composed of orthotropic materials (topaz & barite) and isotropic material (steel) the figures 2 to 7 are drawn between stresses and radii ratios. The standardized values of material constants are mentioned in Table1.

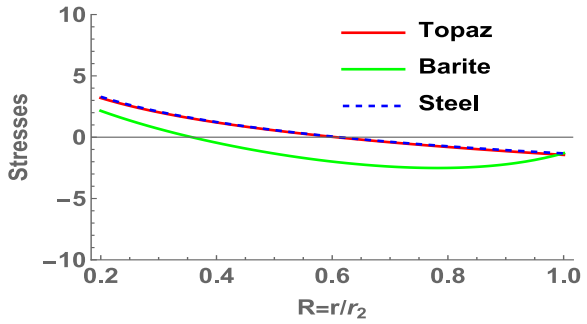

Figure 2: Creep stresses in the spherical shell for orthotropic materials (topaz & barite) and isotropic material (steel) for $n = 1, \theta = 0.5$ & $p = 5$.

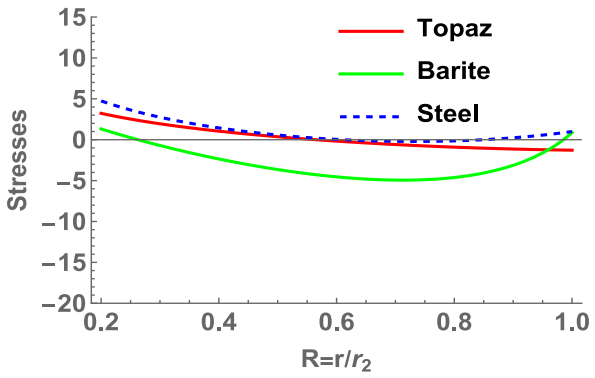

Figure 3: Creep stresses in the spherical shell for orthotropic materials (topaz & barite) and isotropic material (steel) for $n = 1, \theta = 0.5$ & $p = 10$.

ISSN: 2582-7219 | www.ijmrset.com | Impact Factor: 8.206| ESTD Year: 2018|

International Journal of Multidisciplinary Research in Science, Engineering and Technology (IJMRSET)

(A Monthly, Peer Reviewed, Refereed, Scholarly Indexed, Open Access Journal)

Figures 2 and 3 shows the behaviour of circumferential stresses at the creep state in a spherical shell for orthotropic materials (topaz & barite) and isotropic material (steel) for $n = 1, \theta = 0.5$ and different values of $p = 5 \& 10$ respectively. The creep stresses are maximum on the inner surface of the shell compared to the shell's outer surface with the increase in the shell's thickness. If the value of pressure extends from 5 to 10, the stresses in the spherical shell of steel increase, but in case of the spherical shell of topaz and barite, the stresses decrease.

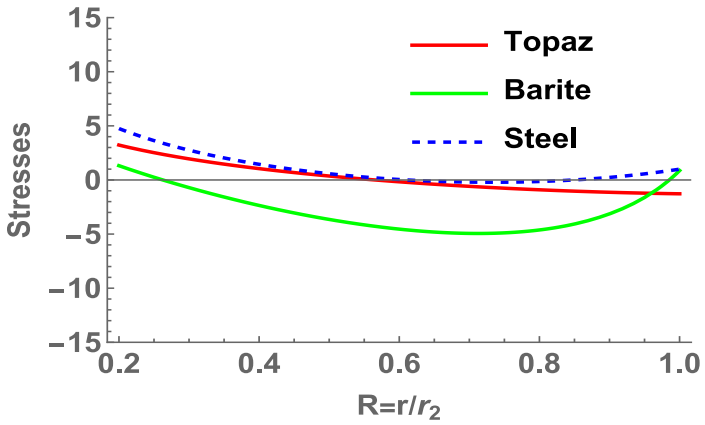

Figure 4: Creep stresses in the spherical shell for orthotropic materials (topaz & barite) and isotropic material (steel) for $n = 1, \theta = 1 \& p = 5$.

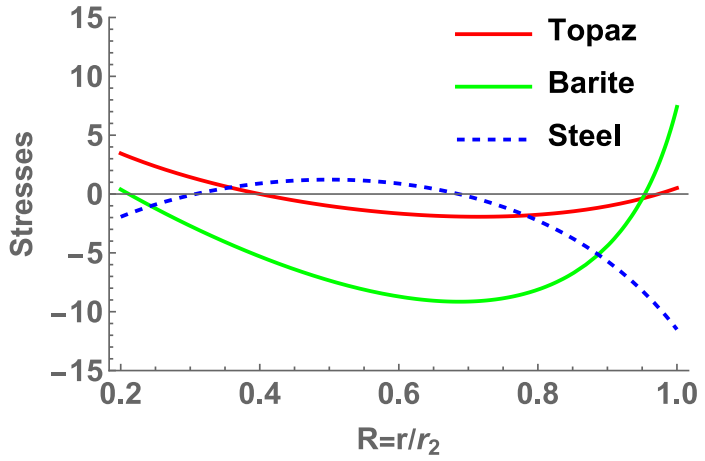

Figure 5: Creep stresses in the spherical shell for orthotropic materials (topaz & barite) and isotropic material (steel) for $n = 1, \theta = 1 \& p = 10$.

Figures 4 and 5 represent the pattern of circumferential stresses at the creep state in a spherical shell for orthotropic materials (topaz & barite) and isotropic material (steel) for $n = 1, \theta = 1$, and different values of $p = 5 \& 10$, respectively. If the value of p extends from 5 to 10, then the stresses in steel are tensile, but in topaz and barite, the stresses are compressive on the mid-surface of the shell.

ISSN: 2582-7219 | www.ijmrset.com | Impact Factor: 8.206| ESTD Year: 2018|

International Journal of Multidisciplinary Research in Science, Engineering and Technology (IJMRSET)

(A Monthly, Peer Reviewed, Refereed, Scholarly Indexed, Open Access Journal)

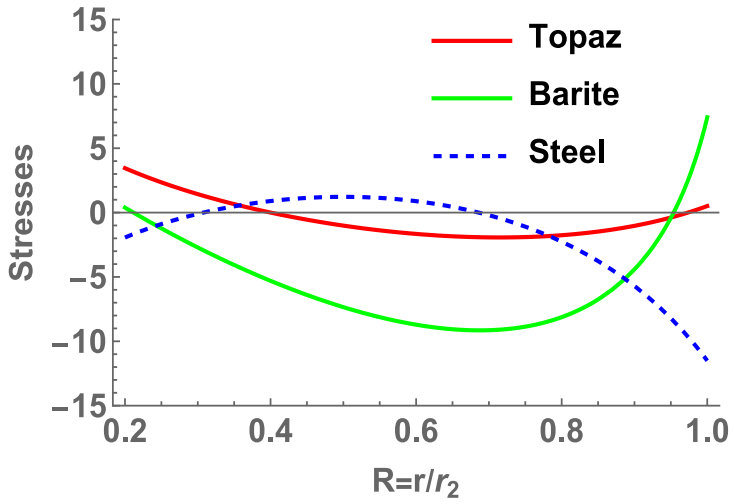

Figure 6: Creep stresses in the spherical shell for orthotropic materials (topaz & barite) and isotropic material (steel) for $n = 1, \theta = 2$ & $p = 5$.

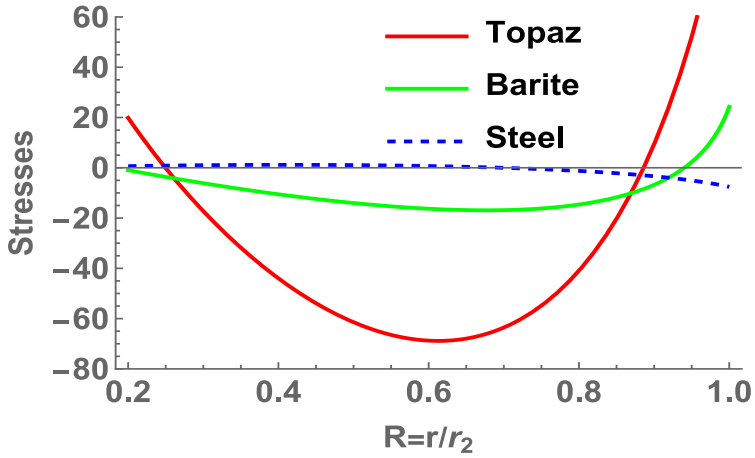

Figure 7: Creep stresses in the spherical shell for orthotropic materials (topaz & barite) and isotropic material (steel) for $n = 1, \theta = 2$ & $p = 10$.

Figures 6 and 7 represent the pattern of circumferential stresses at the creep state in a spherical shell for orthotropic materials (topaz & barite) and isotropic material (steel) for $n = 1, \theta = 2$ and different values of $p = 5$ & 10 respectively. In both topaz and barite, increasing the shell thickness results in greater creep stresses on the outer surface compared to the inner surface. In the case of steel, an increase in shell thickness results in higher creep stresses on the inner surface compared to the outer surface.

It can also be seen that if the value of p extends from 5 to 10, the stresses in topaz are more compressive than the stresses in barite, and the stresses in steel are tensile on the mid-surface of the shell.

VI. SUMMARY AND CONCLUSION

An analytical solution for creep stresses in a spherical shell made of orthotropic material under external pressure is presented using transition theory. The previous study employed the transition theory to investigate elastic-plastic stress concentrations in orthotropic material, which are modelled as spherical shells subjected to a temperature gradient and found that orthotropic shells are useful for engineering purposes. In this study, a comparison has been made between

ISSN: 2582-7219 | www.ijmrset.com | Impact Factor: 8.206| ESTD Year: 2018|

International Journal of Multidisciplinary Research in Science, Engineering and Technology (IJMRSET)

(A Monthly, Peer Reviewed, Refereed, Scholarly Indexed, Open Access Journal)

orthotropic materials (topaz & barite) and an isotropic material (steel) to identify that which is appropriate for engineering design in terms of their strength, durability, and lifespan. Based on graphical and numerical analysis, it is concluded that topaz has compressive stresses and steel has tensile stresses on the mid-surface of the shell.

As a result, it can be inferred that the spherical shell of topaz (orthotropic material) is better for extremely high temperatures without mechanical loading. In contrast, the spherical shell of steel (isotropic material) is more stable in high-pressure and mechanical loading. Spherical shell of orthotropic material topaz can be considered by design engineers in high temperature conditions.

REFERENCES

[1] Seth, B. R. Transition theory of elastic-plastic deformation, creep and relaxation, Nature (1962),195, pp. 896-897 https://doi.org/10.1038/195896a0.
[2] Betton, J. Creep mechanics, Springer, Berlin (2005)
[3] Temesgen, A.G., Singh, S.B., Thakur, P. Modeling of creep deformation of a transversely isotropic rotating disc with a shaft having variable density and subjected to a thermal gradient, Thermal Science and Engineering Progress (TSEP) (2020), Vol. 20, 100745. https://doi.org/10.1016/j.tsep.2020.100745
[4] Saadatfar, M., Babazadeh, A., Babaelehi, M. Stress and Deformation of a Functionally Graded Piezoelectric Rotating Disk with Variable Thickness Subjected to Magneto-Thermo-Mechanical Loads Including Convection and Radiation Heat Transfer, International Journal of Applied Mechanics (2023), 16(01). https://doi.org/10.1142/S1758825124500029
[5] Es-Saheb, M. H., Fouad, Y. Creep Analysis of Rotating Thick Cylinders Subjected to External and Internal Pressure. Analytical and Numerical Approach, Appl. Sci. (2023), 13(21), 11652. https://doi.org/10.3390/app132111652
[6] Sharma, R. Evaluation of thermal elastic-plastic stresses in transversely isotropic disk made of piezoelectric material with variable thickness and variable density subjected to internal pressure, Structural Integrity and Life (2023), Vol. 23, No. 2, pp. 205-212. http://divk.inovacionicentar.rs/ivk/ivk23/205-IVK2-2023-RS.pdf
[7] Sharma, R., Nagar, A. Analytical approach on stress analysis in a functionally graded piezoelectric annular disk with varying compressibility and varying density under internal pressure, International Journal of Non-Linear Mechanics (2024), Vol. 162, 104723. https://doi.org/10.1016/j.ijnonlinmec.2024.104723
[8] Godana., T. A., Singh, S. B., Thakur, P., Kumar, P. Modelling the elastoplastic deformation of an internally pressurized transversely isotropic shell under a temperature gradient, Turkish Journal of Computer and Mathematics Education (TURCOMAT) (2023), Vol. 14, No. 1. https://doi.org/10.17762/turcomat.v14i1.13458
[9] Bayat, S. H., Nazari, M. B. Dynamic crack analysis in anisotropic media under wave-like thermal loading, European Journal of Mechanics – A/Solids (2023), Vol 99, 104913 https://doi.org/10.1016/j.euromechsol.2023.104913
[10] Jafary, H., Taghizadeh, M. Nonlinear dynamics response of porous functionally graded annular plates using modified higher order shear deformation theory, SN Appl. Sci. (2023) 5, 368.https://doi.org/10.1007/s42452-023-05591-6
[11] Vahid Daghigh, Hamed Edalati, Hamid Daghigh, Davy M. Belk, Kamran Nikbin. Time-dependent creep analysis of ultra-high-temperature functionally graded rotating disks of variable thickness, Forces in Mechanics (2023), Vol. 13, 100235, ISSN 2666-3597.https://doi.org/10.1016/j.finmec.2023.100235
[12] Saadatfar, M., Babazadeh, M. A., Babaelahi, M. Thermoelastic creep evolution in a variable thickness functionally graded piezoelectric rotating annular plate considering convection and radiationheat transfer, Mechanics Based Design of Structures and Machines (2023), 1–26. https://doi.org/10.1080/15397734.2023.2266826
[13] Matvienko, O., Daneyko, O., Valikhov, V. Elastoplastic deformation of rotating disk made of aluminium dispersion-hardened alloys, Metals (2023), Vol 13(6), 1028. https://doi.org/10.3390/met13061028
[14] Jafari, N., Azhari, M. Creep instability analysis of viscoelastic sandwich shell panels, Mechanics of Time-Dependent Materials (2024), Vol. 28, pp 65-79.
[15] Park, J. M., Lim, K. Development of axisymmetric shell model for creep deformation analysis of reactor pressure vessel lower head, Nuclear Engineering and Technology (2024), https://doi.org/10.1016/j.net.2024.09.023
[16] Verma, G., Singh, B. Mathematical model of spherical shell under creep deformation, Structural Integrity and Life (2022), Vol. 24, No.1, pp. 65–70.
[17] Shahi, S., Kaur, G., Basker, P. Modelling of creep deformation in an annular rotating disc composed of Si-Ti-C-O fibre-bonded ceramic matrix composite using Seth transition theory, International Journal of Modelling, Identification and Control (2024), Vol. 44, No. 3, pp 246-254. https://doi.org/10.1504/IJMIC.2024.137998

ISSN: 2582-7219 | www.ijmrset.com | Impact Factor: 8.206| ESTD Year: 2018|

International Journal of Multidisciplinary Research in Science, Engineering and Technology (IJMRSET)

(A Monthly, Peer Reviewed, Refereed, Scholarly Indexed, Open Access Journal)

[18] Sharma, S., Panchal, R. Creep stresses in functionally graded rotating orthotropic cylinder with varying thickness and density under internal and external pressure, Structural Integrity and Life (2018), 18(2): 111-119. (http://divk.inovacionicentar.rs/ivk/home.html)

[19] Motameni, A. A parametric study on the elastic limit stresses of rotating variable thickness orthotropic disk, Archive of Applied Mechanics (2024), Vol 94, pp. 737-752. https://link.springer.com/article/10.1007/s00419-024-02548-y

[20] Beheshti, A., Ansari, R. Finite element analysis of compressible transversely isotropic hyperelastic shells, Acta Mechanica (2023), Vol 234, pp. 3061-3079 https://doi.org/10.1007/s00707-023-03536-z

[21] Sharma, R., Nagar, A. Analytical solution of stresses in isotropic disc composed of functionally graded material with variable compressibility and thickness, Structural Integrity and Life (2024), Vol 24, No. 3, pp. 330-336 https://doi.org/10.69644/ivk-2024-03-0330.

[22] Sharma, R., Radakovic, Z. Fracture analysis in an orthotropic rotating hyperbolic disc fitted with stiff rod, Structural Integrity and Life (2024), Vol 24, No. 3, pp. 339-345 https://doi.org/10.69644/ivk-2024-03-0339.

INTERNATIONAL STANDARD SERIAL NUMBER INDIA

INTERNATIONAL JOURNAL OF MULTIDISCIPLINARY RESEARCH

IN SCIENCE, ENGINEERING AND TECHNOLOGY

| Mobile No: +91-6381907438 | Whatsapp: +91-6381907438 | ijmrset@gmail.com |

www.ijmrset.com